RESEARCH PAPER

Design, Development, and Optimization of Oxcarbazepine-Loaded Liposomes with Comparative Evaluation of Their Anti-Epileptic Efficacy in Preclinical Models

Dastagiri Reddy Y*[1] Bhavya Sree P[1], Praveen Kumar Pasala[2], Nitheesha Lingam[3] Mudassir Ahamed S[4]

[1]*Department of Industrial Pharmacy, Santhiram College of Pharmacy, Nandyal, Andhra Pradesh.*
[2.]*Department of Pharmacology, Raghavendra Institute of Pharmaceutical Education and Research, JNTUA, Anantapuramu, Andhra Pradesh 515721, India*
[3]*Department of Pharmaceutics, Santhiram College of Pharmacy, Nandyal, Andhra Pradesh.*
[4]*Department of Industrial Pharmacy, Santhiram College of Pharmacy, Nandyal, Andhra Pradesh.*
Corresponding Author: Y. Dastagiri Reddy. dastu1984@gmail.com,

Received: 16th Dec, 2025; Revised: 8th Feb 2026; Accepted: 12th Feb, 2026; Available Online: 28th Feb, 2026

ABSTRACT
This study aimed to formulate and optimize oxcarbazepine-loaded liposomes using the thin-film hydration technique and Box–Behnken design to increase bioavailability and achieve sustained drug release, addressing the poor aqueous solubility and low oral bioavailability of oxcarbazepine. The BBD evaluated three independent variables, Geolol Mono and Diglyceride (X_1), Glyceryl Tri-stearate (X_2), and Brij S 100 (X_3), on critical responses: entrapment efficiency (%EE), particle size (nm), and zeta potential (mV). Seventeen formulations (F1–F12) were prepared and analyzed. FTIR confirmed that no drug-excipient interactions occurred, whereas FESEM revealed uniform spherical vesicles with smooth surfaces, confirming liposome formation. The optimized formulation contained 213.587 mg of Geolol Mono and Diglyceride, 585.724 mg of glyceryl tri-stearate, and 214.093 mg of Brij S 100, exhibiting 98% entrapment efficiency, 232 ± 42.6 nm particle size, and -62.8 mV zeta potential. The nanometric particle size ensured better cellular uptake and prolonged circulation, whereas a negative zeta potential indicated good physical stability and prevented aggregation. High entrapment efficiency demonstrated effective drug encapsulation. In vitro release studies revealed sustained drug release over 12 h, outperforming the pure drug, with release kinetics following first-order and Fickian diffusion mechanisms, indicating a concentration-dependent diffusion from the lipid bilayer. This study investigated the anticonvulsant and neuroprotective efficacy of OXZ and its novel formulation, OXZL, in a pentylenetetrazole (PTZ)-induced seizure model in rodents. Behavioral seizure parameters, including onset, duration, and motor phases, were evaluated alongside oxidative stress markers (LPO, GSH, GPx, and SOD) in the brain tissue. PTZ treatment significantly ($p<0.001$) induces rapid-onset seizures, increases lipid peroxidation, and suppresses endogenous antioxidant defenses. Compared with OXZ treatment, co-treatment with OXZL provided greater significant ($p<0.001$) protection against seizures, restored the antioxidant status, and improved the viability of CA1, CA2, CA3, DG, and cortex. These findings suggest that OXZL holds promise as a potent antiepileptic agent with antioxidative properties, warranting further mechanistic and clinical evaluation.

Keywords: *Oxcarbazepine, liposomes, thin-film hydration, Box–Behnken design, In vivo.*
How to cite this article: Reddy DY, Bhavya Sree P, Pasala PK, Lingam N, Mudassir Ahamed S. Design, Development, and Optimization of Oxcarbazepine-Loaded Liposomes with Comparative Evaluation of Their Anti-Epileptic Efficacy in Preclinical Models. Int J Drug Deliv Technol. 2026;16(17s): 244-258. DOI: 10.25258/ijddt.16.17s.31

Source of support: Nil.
Conflict of interest: None

**Author for Correspondence: XXX*

Abstract Picture

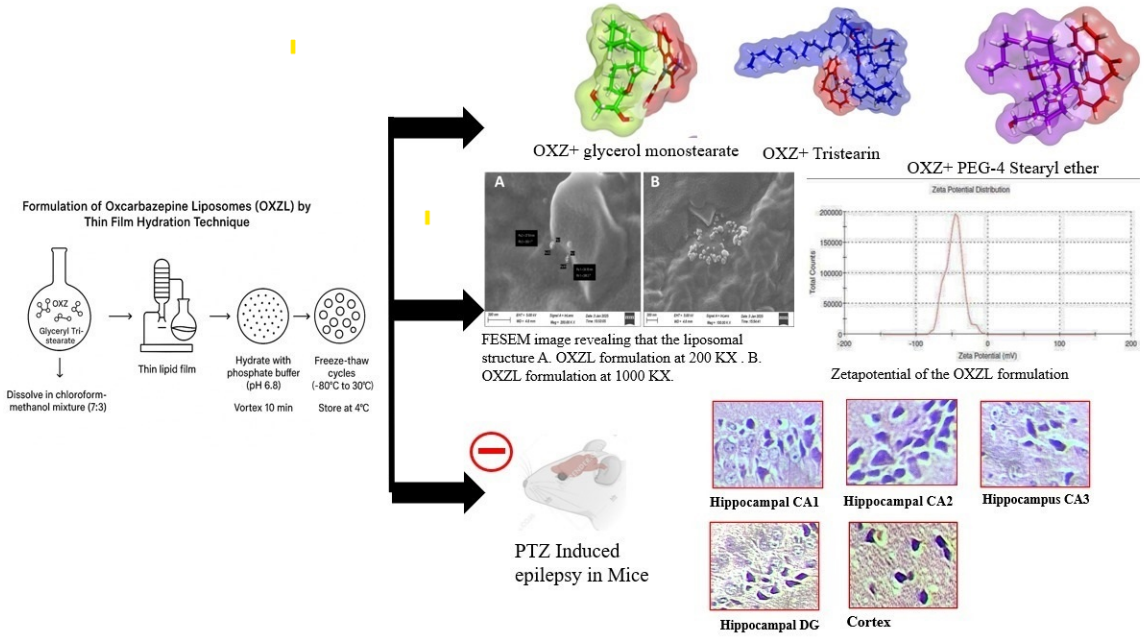

1. INTRODUCTION

Approximately 50 million people worldwide are affected by epilepsy, which is arguably one of the most common chronic neurological diseases[1]. It is characterized by seizures that recur without provocation, hugely affect the quality of life of patients, and place enormous pressure on health systems in communities worldwide[2]. Current antiepileptic drugs (AEDs) control seizures in many patients; however, approximately 30% of patients refuse to respond to existing options available for the management of seizures[3]. This indicates an urgent and persistent need for better-directed treatment.

Oxcarbazepine (OXZ), a second-generation AED, is an important therapeutic option[4]. It is very much liked because of its favorable safety profile and its main mechanism of action for blocking voltage-gated sodium channels to stabilize hyperexcitable neuronal membranes[5]. Nonetheless, the clinical use of OXZ is considerably restricted by its poor aqueous solubility and insufficient pharmacokinetic properties[6]. These factors lead to variable systemic exposures and unpredictable therapeutic responses, which frequently require problematic dosing regimens.

Progressive drug delivery systems must be developed to overcome the pharmacokinetic limitations of OXZ. Advances in liposomal formulations have attracted considerable promise for their value as new vehicles to enhance AED delivery[7]. An improved solvent, a longer time before the whole body clears, and perhaps targeted delivery to the central nervous system (CNS) are desirable criteria in epilepsy therapy[8]. Liposomes are phospholipid bilayers optimized to entrap both hydrophilic and hydrophobic compounds trapped in any one of their compartments, thus giving them a unique ability to deliver poorly water-soluble drugs such as OXZ[9]. The preparation techniques vary, with the thin-film hydration method being recognized for its advantages in producing reproducible and uniform vesicle sizes in formulations[10].

A rational and systematic approach to formulation design is the basis for developing efficient complex liposomal formulations[11]. Factorial designs, especially the Box—Behnken design (BBD), are excellent statistical tools for optimizing complex formulations by allowing the efficient deduction of the effects of the levels of multiple and independent variables and their interactions on the critical quality attributes for liposome formulation[12]. With respect to liposomal drug delivery, formulation parameters, such as lipid composition, surfactant concentration, and preparation conditions, markedly influence key characteristics.

However, AEDs that possess intrinsic neuroprotective capabilities are now generally recognized, in addition to improving drug delivery and seizure control. The modern conception of the pathophysiology of epilepsy is that neuronal hyperexcitability is not the only factor; it includes progressive neurodegenerative processes, even within the nervous system[13]. These long-lasting changes are often wrought through intertwined mechanisms such as oxidative stress and neuroinflammation[14]. These mechanisms greatly contribute to the associated permanent cognitive and behavioral deficits caused by epilepsy. These are necessary requirements for the development of any alternative therapy that is useful: addressing the underlying neurodegenerative aspects of disease modification beyond suppressing seizure activity.

The pentylenetetrazole (PTZ)-induced seizure model is perhaps one of the most widely adopted and well-validated experimental systems for research into critical aspects of epilepsy pathophysiology, including some of the mechanisms mentioned[15]. This model consistently elicited acute seizure activity through GABAergic neurotransmission blockade. Importantly, PTZ also induces

significant oxidative damage to the brain tissue; thus, it can be considered neurodegenerative with respect to the properties associated with chronic epilepsy[16]. Thus, it has become a valuable and comprehensive model for evaluating both anticonvulsant activity and any neuroprotective advantages that may be associated with candidate therapeutic agents.

The present investigation aimed to address the urgent problems associated with therapeutics for epilepsy to formulate and characterize the optimized liposomal formulation of OXZ. Using systematic factorial design approaches, attempts were made to rationally identify and optimize significant formulation parameters for the desirable physicochemical properties of OXZ-loaded liposomes. The formulation was studied in standard in vivo seizure models for its therapeutic efficacy, including anticonvulsant activity and probable neuroprotection against degenerative processes. Thus, the present study represents a holistic approach against limits set by conventional formulations of OXZ therapy, broadening the future perspective for integrating better drug delivery potential with the potential for neuroprotection in an innovative approach to improving epilepsy management.

2. MATERIALS & METHODS

2.1. Molecular Docking

A docking study was undertaken in AutoDock Vina (v.1.2.3) (Trott & Olson, 2010) to elucidate the molecular interactions underlying the extraordinarily high entrapment efficiency and sustained release of oxcarbazepine (OXZ) in the optimized liposomal formulation. The 3D structure of OXZ (PubChem CID: 34312) was retrieved from PubChem, and the liposomal components were modeled as analogs: glycerol monostearate (geolol surrogate, CID: 24699), tristearin (glycerol tristearate analog, CID: 11146), and PEG-4 stearyl ether (Brij S 100). Ligands and polymers were energy-minimized (MMFF94 force field) in Avogadro (v. 1.2.0), whereas the docking grids were centered on the entire polymer structure to allow for flexible binding sites (Table 1). The affinity scores (kcal/mol) and RMSD values (lower/upper bounds) were calculated for the top nine binding modes[17, 18].

2.1 Chemicals and reagents

Glyceryl tristate and Brij S100 were purchased from Sigma—Aldrich (St. Louis, MO, USA). Oxcarbazepine was obtained from Yarrow Chemical Products (Mumbai, India). Geleol monoglyceride was provided by Gattefosse India Pvt., Ltd. Mumbai, india. Methanol, chloroform, disodium hydrogen phosphate, and potassium hydrogen phosphate were obtained from Merck (Mumbai, India).

A Box–Behnken design [19] employed to optimize the concentrations of glycol monoglyceride, glycerol tristearate, glycerol, and Brij S100 for OXZ-loaded liposomes, focusing on three key responses: entrapment efficiency (Y1), particle size (Y2), and zeta potential (Y3), which are critical for determining the drug dosage regimen. Liposomes were formulated with various molar ratios of the three components to explore the design space using Design Expert 13.0.0 software (Stat-Ease Inc., USA). The independent variables Geleol mono diglyceride glyceryl (X1), Glyceryl Tristearate (X2), and Brij S100 (X3) were assessed at two levels (low and high). Data from 17 experimental runs were analyzed via ANOVA to statistically validate the model. The optimal model was selected based on R^2, F value, p value, CV, adjusted and predicted R^2, and adequate precision metrics (Table 2). Contour and 3D response surface plots were generated to identify optimal formulation conditions [20, 21].

2.2 Formulation of Oxcarbazepine Liposomes (OXZLs) via the Thin Film Hydration Technique

Liposomes were prepared using a thin layer hydration method. OXZ, glycerol tristearate, glycol mono- and diglycerides, and Brij S100 were dissolved in a chloroform-methanol mixture (7:3) at a 1:0.5:0.75 molar ratio and transferred to a 100 mL round-bottom flask. The solvent was evaporated under vacuum using a rotary vacuum evaporator at 70°C and 100 rpm to form a thin lipid film. To ensure complete solvent removal, vacuum was maintained. The dried lipid film was hydrated with phosphate buffer (pH 6.8), vortexed for 10 min, and subjected to three freeze—thaw cycles (-80°C to 30°C). The final liposomal formulation was stored at 4°C for further analysis[22].

2.3. Evaluation Parameters

2.3.1. FTIR Studies

FTIR analysis was conducted on both the pure drug and the optimized formulation using the potassium bromide (KBr) pellet method. In this approach, the pure drug and lyophilized optimized formulation were thoroughly blended with KBr in a 1:10 ratio. The mixtures were then finely ground to ensure their uniformity. A small portion of the resulting powder was subjected to high pressure to form thin semitransparent pellets. The infrared spectra of these pellets were analyzed over the range of 500--4000 cm^{-1} via an FTIR spectrophotometer[23].

2.3.2. Entrapment efficiency:

Entrapment efficiency was estimated by measuring the concentration of the unloaded drug in the dispersion medium. Oxcarbazine liposome samples were prepared and placed in centrifuge tubes. The liposomes were separated from the medium via centrifugation at 10,000 rpm at -4°C for 15 min. The clear liquid supernatant (if not) was diluted (manner) with buffer, and the samples were measured with a UV–visible spectrophotometer (SHIMADZU) at the appropriate nanometer scale for each drug. A. A. Date 2011.

$Total$ amount of $Drug$ – Amount of $Free\ Drug$/Total amount of drug X100

2.3.3. Particle size and zeta potential:

Dynamic light scattering at 25°C was employed to measure particle size and zeta potential using a Malvern Zetasizer (Mastersizer 2000, Malvern Instruments, UK). Dilute liposome samples (minimum 0.9 mL) were filled with disposable zeta cells and measured at a 90° scattering angle. Probe sonication was employed to avoid interference, and measurements were performed in triplicate to ensure accuracy. This approach was employed to perform a

statistical analysis to observe variations in the results.[24, 25].

2.3.4. Surface Morphology by Field Emission Scanning Electron Microscopy:

The surface morphology and size of the liposomes were analyzed using field emission scanning electron microscopy (FESEM). To improve the conductivity of the sample, an aluminum stub with conductive carbon tape and a thin gold/platinum layer was prepared and placed on the stub. High-resolution micrographs of the particle shape, surface characteristics, and structural integrity were captured under optimal conditions using secondary electron detector imaging.

2.4. **In Vitro Diffusion Studies**

An in vitro drug permeation study was performed using Franz diffusion cells (20 mL receptor volume with a surface area of 3.14 cm^2). Phosphate buffer (pH 6.8) was added to the receptor chamber, which was continuously stirred using a magnetic stirrer and maintained under sink conditions. The air bubbles were carefully removed from the donor and receptor compartments, and the two compartments were separated using a 2 × 2 cm^2 activated cellophane membrane. To maintain the temperature at 37 ± 0.5°C, a circulating water bath was used in the donor compartment, 2 mL of an OXZ-loaded liposomal formulation equivalent to 10 mg OXZ was transferred, and 2 mL samples were withdrawn from the receptor chamber at intervals of 1, 2, 3, 4, 6, 8, and 10 h and replaced with fresh buffer. Three replicates were performed for each sample. The optimized liposomal batch was quantitated (permeation) with OXZ over time using a validated UV spectroscopy technique, and the % drug release was plotted.9

2.5. Stability studies of OXZ-loaded Liposomes

The physical stability of the optimized liposomal formulation was evaluated under two storage conditions of 5 °C ± 3 °C and 25 °C ± 2 °C/60% RH ± 5% for 6 months at 5 ± 3 °C and 25 ± 2 °C/60% RH ± 5% room temperature in accordance with ICH Guideline Q1A(R2). Tightly sealed 10 mL glass vials containing the formulation were stored at specified temperatures. Samples were taken at intervals of 0, 3, and 6 months for analysis of the output of various physical parameters, such as drug leakage, particle size, vesicle aggregation, zeta potential, and percentage drug entrapment. Additionally, the vesicles were microscopically observed for changes in their size and aggregation behavior.

2.6. Animals

Wistar rats (200–220 g) were housed under standard laboratory conditions (25 ± 2°C, 12:12 h light/dark cycle), with free access to food and water. All procedures were approved by the Institutional Animal Ethics Committee (IAEC) and adhered to IAEC/VII/04/RIPER/2025.

2.7. Seizure Induction

PTZ was freshly prepared by dissolving it in cold normal saline and was administered at a dose of 60 mg/kg i.p. 6 h after drug administration. This dose of PTZ was standardized as 100% convulsive dose, with the minimum death rate observed in rats in our laboratory. Latency to myoclonic jerks was noted along with the occurrence of generalized tonic-clonic seizures (GTCSs). Loss of the righting reflex was also monitored. The observation period was 30 min for individual mice[26].

Mice were randomly distributed into four groups (n = 6/group):

Group I, control group: mice received a daily oral dose of 0.9% NaCl for 14 days. On Day 14, the rats were injected intraperitoneally (i.p.) with 0.9% NaCl 1 h after the oral administration of saline.

Group II (PTZ): Mice received a daily oral dose of normal saline for 14 days. On Day 14, the animals received a single i.p. injection of PTZ (60 mg/kg) to induce acute epileptic seizures 1 h after the oral administration of saline, as described by Abdel-Rahman et al.[27].

Group III, OXZ + PTZ-treated group: Mice received a daily oral dose of OXA (16 mg/kg) for 14 days based on the methodology described by Arafa et al.[28]. On Day 14, mice received a single i.p. injection of PTZ (60 mg/kg) 1 h after OXA administration.

Group IV, OXZL + PTZ-treated group: Mice received a daily oral dose of OXAL (16 mg/kg) for 14 days. On day 14, mice received a single i.p. injection of PTZ (60 mg/kg) 1 h after OXAL administration.

2.8. Behavioral Record

The mice were monitored for 40 min after PTZ injection, and the seizure index score was determined based on the revised Racine et al. [29]as follows:

0, no behavioral change, 1 = Whisker trembling, 2 = Facial jerking, 3 = Neck jerking, 4 = Clonic seizures; 5, lying on the side and wild jumping; and 6, death. Additionally, the duration of the seizures was recorded.

2.8.1. ***Oxidative Stress index evaluation:*** Malondialdehyde (MDA) was assessed to reflect the level of lipid peroxidation using the thiobarbituric acid method described by Ohkawa et al. 1979[30].

2.8.2. ***Antioxidant Activity Assessment:*** The hippocampal activity of glutathione peroxidase (GPx) was assessed according to the procedures described by Paglia et al.*[31]*. The hippocampal SOD activity was determined at 480 nm using the technique described by Misra et al.*[32]*.

2.8.3. ***Histopathological Examinations:*** Brains were fixed in 10% neutral buffered formalin, dehydrated, and paraffinized at room temperature for 24 h, followed by sectioning (4–5 μm). The sections were stained with hematoxylin and eosin for light microscopy.

2.9. Statistical Analysis

Data are expressed as mean ± SEMs. Statistical significance was evaluated by one-way analysis of variance (ANOVA) followed by Tukey's multiple comparison test using GraphPad Prism 9.0. Statistical significance was set at $p < 0.05$.

3. RESULTS

3.1. Molecular Docking

The docking approach revealed the binding affinities of the oxcarbazepine and liposomal components. Oxcarbazepine showed the strongest binding with glycerol monostearate (ΔG = -7.6 kcal/mol), implying the presence of hydrogen bonds between the amide/carbonyl groups of the drug and the hydroxyl groups of glycerol. The binding was moderate for tristearin (ΔG = -6.7 kcal/mol), with hydrophobic interactions likely occurring between the aromatic rings of OXZ and the alkyl chains of the lipid. For PEG-4 stearyl ether (Brij S 100), the binding affinity was the weakest (ΔG = -4.5 kcal/mol), which aligns well with its role as a stabilizer of the particle surface rather than one of the major drug-load-bearing components (Figure 1).

3.2. FTIR Studies

The O–H stretching absorptions occur at 3354.52 (cm^{-1}) and 3190.50 (cm^{-1}), and the peaks at 1673.77 (cm^{-1}), 1639.67 (cm^{-1}) and 1062.73 (cm^{-1}) are characteristic of the functional groups of oxcarbazepine. These peaks are at 3468.75 cm^{-1}, 2884.82 cm^{-1} and 2916.01 cm^{-1} for glyceryl tristearate, Geleol mono- and diglycerides, and Brij S100, which represent alkanes, alcohols, and aliphatic ethers, respectively. More importantly, the lack of significant shifts and loss of typical peaks indicated that there was no chemical interaction between oxcarbazepine and the excipients; hence, the formula was physically compatible and stable (Figure 2).

The optimization study explored the effects of three independent variables (A, B, and C) on the key formulation responses: entrapment efficiency (Y1), particle size (Y2), and zeta potential (Y3). The final coded equations and the corresponding 2D contour and 3D response surface plots provided critical insights into the behavior of the system.

3.3. Entrapment Efficiency:

The contour plot displays the entrapment efficiency (%) based on two variables: A (gall mono- and diglycerides in mg) on the x-axis and B (glycerol tristearate in mg) on the y-axis. A ranges from approximately 179.18 mg to 268.77 mg, whereas B ranges from 445.74 mg to 668.61 mg. Maximum entrapment efficiency (~91.7%) and minimum efficiency (~80.3%) were observed, indicating a synergistic interaction between the two variables.

This 3D surface plot illustrates the combined influence of Geleol Mono and Diglycerides (A) and Glyceryl Tristearate (B) on entrapment efficiency, with the third factor (C) fixed at 195.96 mg. The X-axis (A) ranges from approximately 179.18 to 268.77 mg, and the Y-axis (B) ranges from 445.74 to 668.61 mg, whereas the Z-axis reflects an entrapment efficiency (%) ranging from approximately 80.3% to 91.7%. The plot reveals that entrapment efficiency increases progressively with increasing levels of both A and B, reaching its peak at higher concentrations of both variables. A distinct interaction between A and B is evident, as shown by the curved surface trending upward toward the upper-right region. This curvature suggests a linear yet synergistic relationship between the variables and efficiency.

Final Equation in Terms of Coded Factors (Y1) Entrapment efficiency (%): +80.30+1.45*A+1.85*B+1.25*C+3.22*AB+2.63 AC+0.8750* BC+9.26 *A^2+4.16*B^2+3.81*C^2

3.4. Particle size (nm)

The counter plot illustrates that smaller particles (~186 nm) formed at high Geleol Mono values and low Glyceryl Tristearate values, whereas larger particles (~637 nm) had the opposite effect. The plot aids in optimizing the component levels for the desired particle sizes (Figure 3).

This image shows a 3D surface plot used to visualize the effects of two variables, A: Geleol Mono and Diglycerides (mg) and B: Glyceryl Tristearate (mg), on the response variable, which is the particle size (nm). X-axis (A): Geleol mono- and diglycerides (mg), ranging from approximately 445.74 mg to 2687.7 mg. Y-axis (B): glyceryl tristearate (mg), ranging from approximately 534.888 mg to 668.61 mg. Z-axis: Particle size (nm), ranging from approximately -400 nm to 800 nm (note: negative values for particle size are not physically meaningful but may result from the mathematical model fit). Surface shape: The plot shows how particle size varies with changes in the two lipid components. The surface was curved, indicating a nonlinear relationship.

Final Equation in Terms of Coded Factors (Y2) Particle size (nm): +466.00--14.38*A-64.00*B-18.62*C-46.75*AB-48.50*AC-22.25*BC-157.00*A^2--20.75*B^2--11.50*C^2

3.5. Zetapotential (mV)

The contour plot illustrates how varying the concentrations of Geleol Mono and Diglycerides (A) and Glyceryl Tristearate (B) affect the zeta potential, a key indicator of colloidal stability. Deep blue regions (approximately -62.8 mV) occurred at low levels of both A (~179.18 mg) and B (~445.74 mg), indicating high stability. In contrast, the highest zeta potential (red, up to 38.6 mV) was observed when B was high (~668.61 mg) and A remained low (~179.18 mg). Intermediate values (green/yellow) lie between these extremes, with smooth transitions marked by contour lines labeled -53 to -13 mV (Figure 4).

Zeta potential varies significantly with changes in the concentrations of Geleol Mono and Diglycerides (A) and Glyceryl Tristearate (B). The maximum zeta potential (positive value) was observed at the corners where either A or B was at its maximum. The minimum zeta potential (negative value) was observed at the opposite corners. The surface was almost planar, indicating a linear or near-linear relationship between these variables and the zeta potential within the tested range. Blue (-62.8 mV) indicates the lowest zeta potential values. Green (38.6 mV) indicates the highest zeta potential values.

Final Equation in Terms of Coded Factors (Y3) Zetapotential (mV): -27.67--4.19*A+7.73*B--3.09*C--23.85*AB--0.8250*AC+16.50*BC

The FESEM image revealed that the liposomal structure had a smooth spherical morphology, uniform distribution, and good formula. This lipid bilayer appears to be compatible with low aggregation for efficient encapsulation and release of drugs. The measured nanoscale sizes ranged from small unilamellar vesicles (2 nm) to possible

multilamellar structures (135.7, with an average size of 241.7 nm) (Figure 5). The optimal formulation was confirmed by intact vesicles, and correspondingly improved drug delivery efficiency and bioavailability.

ANOVA results showed good R^2 and R^2 values adjusted for EE (98% and 96%), mean size (97% and 91%), and zeta potential of the produced oxcarbazepine liposomes (99% and 97%, respectively). The high-adjusted R-squared value demonstrates a strong correlation between the estimated and measured values, which verifies the accuracy of the data and the model.

The "lack of fit" *p* values for the mean size, EE and zeta potential were 0.3186, 0.0728, and 0.3234, respectively. These values were all greater than 0.05, indicating that the lack of fit was not significant compared with the pure error, and that the model correctly predicted the experimental data. Figure S1 shows how well the EE, particle size, and zeta potential values fit the expected values. These results demonstrate that the model created in this study can correctly project the experimental data. Notably, zeta potential was used to measure the stability of liposomes in suspension; values higher than 30 mV indicate liposome stability. The generated oxcarbazepine liposomes exhibited good stability in this study, and ZP was always greater than −30 mV.

3.6. Stability Studies

At 5 ± 3 °C, the liposomal formulation demonstrated good physical stability for over 6 months. Minimal changes in particle size, zeta potential, and entrapment efficiency, with negligible drug leakage or vesicle aggregation, were observed. At 25 ± 2 °C/60% RH ± 5%, slightly more pronounced physical changes were observed, including a moderate increase in the particle size, drug leakage, and reduced entrapment efficiency. However, the changes were still within acceptable limits, indicating that the formulation remained physically stable for over 6 months at room temperature.

The epileptic seizure parameters recorded in the present study were significantly different between the treatment groups, demonstrating the potential efficacy of oxcarbazepine-loaded liposomes (OXZLs) in mitigating seizures induced by pentylenetetrazole (PTZ) in rodents. A comparison of the onset, duration, and individual seizure phases (flexion, extension, and clonus) provided valuable insights into the anticonvulsant and neuroprotective effects of these treatments. The onset of seizures was further delayed to 7.3 ± 0.01 minutes, with OXZL providing the most significant delay in seizure onset. This demonstrates the enhanced anticonvulsant efficacy of the liposomal formulation, likely due to the better bioavailability and prolonged circulation time of the drug. The seizure duration was significantly reduced to 4.5 ± 0.02 minutes, indicating that the OXZ-loaded liposomes provided a more substantial protective effect, likely due to improved drug delivery and sustained release**.** This result is in line with previous findings that liposomal formulations enhance the therapeutic effects of poorly soluble drugs[33]. The duration of the flexion phase was significantly reduced to 0.2 ± 0.1 minutes, indicating that OXZL is highly effective in reducing the intensity and duration of this seizure phase. The substantial reduction in flexion time further highlights the superior neuroprotective effects of OXZL, potentially owing to its antioxidant properties. The extension phase was significantly reduced to 2.1 ± 0.3 minutes, showing that the liposomal formulation (OXZL) is far more effective than OXZ alone in reducing the severity of seizure manifestations. The clonus phase was further reduced to 0.3 ± 0.2 minutes, demonstrating the superior efficacy of OXZL in controlling motor seizures. This reduction aligns with the ability of liposomal formulations to provide prolonged therapeutic effects via slow drug release[34].

3.7. Effect on Seizures

The PTZ-induced seizure model effectively elicited convulsive episodes in all the mice. This confirms its reliability as a model of generalized seizures. In the PTZ-only group, seizures manifested rapid onset (0.15 ± 0.001 min), prolonged duration (24.3 ± 0.2 min), and robust motor phases, including flexion, extension, and clonus. In contrast, co-treatment with OXZ significantly delayed seizure onset (4.3 ± 0.02 min), reduced seizure duration (20.3 ± 0.03 min), and attenuated the motor seizure phase. Notably, OXZL treatment provided complete protection, with no seizures observed in treated animals, a marked delay in onset (7.3 ± 0.01 min), and a substantial reduction in motor activity scores (Table 3).

3.8. Hippocampal Biomarkers

To further elucidate the protective mechanisms of OXZ and OXZL, we quantified key oxidative stress biomarkers in the brain homogenates.

3.8.1 Lipid peroxidation (LPO): PTZ-treated animals presented a significant increase in LPO levels (4.5 ± 0.3 nmol/mg protein, $p<0.001$), indicating elevated membrane lipid peroxidation and oxidative injury. OXZ treatment partially reduced LPO levels (3.2 ± 0.4 nmol/mg, $p<0.001$), whereas OXZL treatment led to a greater reduction (2.1 ± 0.3 nmol/mg, $p<0.001$), indicating a stronger antioxidant effect (Figure 6A).

3.8.2. Reduced glutathione (GSH): PTZ administration significantly depleted GSH (0.22 ± 0.05 nmol/mg protein, $p<0.001$), reflecting impaired redox homeostasis. Both OXZ (0.36 ± 0.04 nmol/mg, $p<0.001$) and OXZL (0.45 ± 0.05 nmol/mg, $p<0.01$) improved GSH levels, with OXZL showing superior restoration toward normal values (0.68 ± 0.03 nmol/mg in controls) (Figure 6B).

3.8.3. Glutathione peroxidase (GPx) **activity:** GPx activity was significantly lower in the PTZ group (10.1 ± 0.8 U/mg protein, $p<0.001$) than in the normal group (22.5 ± 0.7 U/mg). OXZ (15.3 ± 0.6 U/mg, $p<0.001$) and OXZL (18.7 ± 0.9 U/mg, $p<0.001$) significantly enhanced GPx activity, with the latter closely approximating control values (Figure 6C).

3.8.4 Superoxide Dismutase (SOD) Activity: SOD activity also declined sharply following PTZ treatment (790 ± 40 U/mg protein, $p<0.001$), but improved with OXZ (1210 ± 60 U/mg, $p<0.001$) and was more robust with OXZL (1475

± 50 U/mg, $p<0.001$), again suggesting a more pronounced antioxidative effect of OXZL (Figure 6D).

3.13. Histopathology

In normal mice, CA1, CA2, and CA3 contain densely packed pyramidal neurons with an intact morphology. PTZ treatment causes neuronal shrinkage, pyknotic nuclei, perineuronal spaces, and necrotic and apoptotic cell death. OXZ co-treatment partially restored architecture and reduced neuron loss, whereas OXZL likely resulted in greater preservation of CA1, CA2, and CA3 pyramidal neurons. In normal mice, the dentate gyrus has intact molecular, granular, and polymorphic layers. PTZ induces granule layer thinning, neuronal shrinkage, halo formation, and astrocyte proliferation. OXZ partially restores the layer thickness and reduces degeneration, whereas OXZL is expected to provide greater histological preservation and further reduce neuronal damage. In normal mice, the cortex exhibits healthy lamination and a uniform cell distribution. PTZ treatment causes apoptosis and neuronal loss. Co-treatment with OXZ markedly reduced PTZ-induced apoptosis and morphological damage. Compared with OXZ alone, the combination of PTZ + OXZL is presumed to provide even greater neuroprotection and mitigation of cortical damage owing to enhanced anti-inflammatory and neuroprotective effects (Figure 7).

4. DISCUSSION

Molecular docking studies have depicted the interaction patterns of oxcarbazepine with liposomal constituents, thereby providing a molecular explanation for why the formulation performed better. The binding affinities established distinctions between liposomal components in their respective roles.

Glycerol monostearate was found to bind strongly to oxcarbazepine, and this interaction correlated well with the very high drug-loading capacity of the formulation. This high affinity is due to hydrogen bonding between the polar functional groups of the drug and the hydroxyl groups of glycerol, thus facilitating stable drug incorporation within the lipid bilayer[35, 36]. The high entrapment efficiency observed in the experiments may be attributed to these molecular interactions. The moderate interaction of oxcarbazepine with tristearin reflects the relevance of hydrophobic forces in ensuring that drug retention occurs inside the liposomal core[37]. This molecular trend governs sustained drug release from formulations, in which the slow diffusion of drug molecules through the lipid matrix is bound by hydrophobic interactions. On the other hand, relatively weak interactions with PEG-4 stearyl ether (Brij S 100) seem to explain its function as a stabilizer on the liposomal surface as a stabilizer[38]. In other words, the weak binding affinity allows the PEG chains to unfold into the aqueous phase, thus providing steric hindrance against particle aggregation. This molecular organization explains the excellent colloidal stability resulting from the high negative zeta potential.

The docking study correlated well with and was strengthened by FTIR analysis, where characteristic spectral changes pertaining to non-covalent interactions without chemical drug modification were observed. Hence, they jointly sketch a consistent survival strategy depicting how molecular-level interactions translate into macroscopic formulation attributes.

These computational studies show a compromise that justifies further optimization of the formulation; each logged component performs a particular yet complementary function, namely glycerol monostearate for drug loading, tristearin for release performance, and Brij S 100 for physical stability. Such an understanding at the molecular level is an excellent starting point for advancing the next generation of liposomal drug delivery systems for poorly soluble drugs, such as oxcarbazepine.

The present study aimed to enhance the bioavailability and sustained release of oxcarbazepine (OXZ) by formulating and optimizing OXZ-loaded liposomes via the thin-film hydration technique combined with a 2^3 factorial design. This study specifically focused on improving the poor aqueous solubility and low oral bioavailability of OXZ, which is a longstanding challenge for many anticonvulsant drugs including OXZ (Nassir et al., 2020). By carefully selecting and optimizing the key formulation variables Geolol Mono and Diglyceride (X_1), Glyceryl Tri-stearate (X_2), and Brij S 100 (X_3), the study achieved a formulation with high entrapment efficiency (98%), a particle size of 232 ± 42.6 nm, and a negative zeta potential (-62.8 mV). These characteristics are crucial for improving cellular uptake, prolonging circulation, and physical stability[39]**.** The FESEM images revealed uniform spherical vesicles with smooth surfaces, which corresponded to the formation of a stable nanostructured liposomal system. These results are in line with a number of earlier studies that demonstrated that liposomal formulations are capable of markedly improving the pharmacokinetic profile of poorly soluble drugs by enhancing their drug delivery and stability Anjali PB 2024[33].

The optimized OXZ-loaded liposomes (OXZLs) showed a sustained in vitro drug-release profile over 12 h. The release kinetics followed a first-order and Fickian diffusion mechanism, and drug diffusion from the lipid bilayer followed a concentration-dependent mechanism. Similar to other liposomal formulations, this controlled drug release pattern is typical for liposomal formulations that encapsulate an active compound within an aqueous lipid membrane to entrap it within the matrix, extend the release time, and increase its bioavailability[40].

In addition to improving bioavailability, the anticonvulsant and neuroprotective efficacy of OXZL was evaluated in a pentylenetetrazole (PTZ)-induced seizure model in rodents. Behavioral seizure parameters demonstrated that OXZL offers superior protection over OXZ in reducing both the onset and duration of seizures as well as in mitigating the severity of the motor phases (flexion, extension, and clonus). The liposomal formulation of oxcarbazepine significantly delayed the onset of seizures and shortened the duration and severity of seizure phases, suggesting that OXZL has a more potent anticonvulsant effect. This could be attributed to the improved pharmacokinetics and

enhanced drug delivery of the liposomal formulation, which ensures better bioavailability, sustained release, and targeted drug action in the brain[40]. PTZ administration also results in increased lipid peroxidation and reduced levels of antioxidants such as glutathione (GSH) and superoxide dismutase (SOD), which are well-established markers of oxidative stress in epilepsy, in the brain[41]. However, OXZL provided a more robust protection against seizures and completely restored the antioxidant defense system, as evidenced by the significant restoration of GSH, GPx, and SOD levels, indicating superior therapeutic efficacy. These results are in agreement with studies that suggest that liposomal formulations not only improve drug delivery, but also enhance pharmacodynamic effects, potentially reducing the side effects associated with conventional drug formulations[42].

The neuroprotective effect of OXZL is also supported by its antioxidant properties, which are essential for the management of oxidative stress in seizure disorders. Oxidative stress has been implicated in the pathophysiology of epilepsy, and the ability of OXZL to restore endogenous antioxidant levels further underscores its potential as a dual-action therapeutic agent that provides both anticonvulsant and neuroprotective effects[43]**.** Histological data revealed that the pentylenetetrazol (PTZ) model of induced seizures causes neuronal degeneration marked by shrinkage, pyknotic nuclei, neuronal loss, and apoptosis in the hippocampal subfields CA1, CA2, CA3, dentate gyrus (DG), and cortex. These histological changes reflect neurotoxicity and gliosis, respectively. Co-treatment with oxcarbazepine (OXZ) partially restored neuronal morphology, reduced the expression of apoptotic markers, and preserved neuron number despite volume loss, indicating a neuroprotective effect. Emerging evidence suggests that the oxcarbazepine-lamotrigine combination (OXZL) may provide enhanced neuroprotection, further attenuating neuronal loss and morphological damage by more effectively reducing oxidative stress and inflammation, thereby preserving hippocampal and cortical structures better than PTZ or PTZ+OXZ alone, which is supported by previous scientific data[44, 45]. The complete seizure protection provided by OXZL, coupled with its favorable antioxidant profile, highlights its potential for further clinical evaluation, especially in the management of refractory epilepsy, which remains a significant challenge in clinical practice.

5. CONCLUSION

In summary, OXZ-loaded liposomes significantly improved the bioavailability, sustained release, and neuroprotective efficacy of oxcarbazepine. The liposomal formulation (OXZL) exhibited a high entrapment efficiency, favorable particle size, and excellent physical stability, leading to enhanced drug delivery and prolonged therapeutic action. Furthermore, OXZL provided substantial protection against PTZ-induced seizures and oxidative stress, indicating its potential as a potent anti-epileptic agent with antioxidative properties. These findings suggest that OXZL could be a promising approach for improving the treatment of epilepsy and other neurological disorders, warranting further mechanistic investigation and clinical trials.

Ethics Approval

All experimental procedures and protocols were approved by the Institutional Animal Ethics Committee (IAEC) of RIPER (Approval Number: IAEC/VII/04/RIPER/2025) and were performed in accordance with relevant guidelines and regulations.

Consent for Publication

All authors agree with the final version of this manuscript and with its current submission.

Competing Interests

The authors have no relevant financial or non-financial interests to disclose.

Funding

This project was not funded.

Acknowledgements: The authors express their gratitude to the management of Santhiram College of Pharmacy, Nandyal, Andhra Pradesh, and Raghavendra Institute of Pharmaceutical Education and Research, JNTUA, Anantapuramu, and Andhra Pradesh for providing the facilities for conducting the research. DST FIST for provided laboratory facilities.

Data Availability Statement:

Table 1: Docking grid parameters used for the molecular docking of oxcarbazepine with selected pharmaceutical polymers.

Polymer	Center X	Center Y	Center Z	Size X	Size Y	Size Z
Glycerol Monostearate (Geolol surrogate)	-0.34412	0.10804	-0.25124	15	15	15
Tristearin (Glyceryl Tristearate analog)	0.86086	2.649653	-0.79235	15	15	15
PEG-4 Stearyl Ether (Brij S 100)	0.35218	-0.04179	0.464611	15	15	15

Table 2: Summary of the design of oxcarbazepine liposomes by using the Box–Behnken design

SNO	Space Type	X1 Geleol Mono and Diglycerides	X2 Glyceryl Tristearate	X3 Brij S100	Y1 Response Entrapment Efficiency (%)	Y2 Response Particle Size (nm)	Y3 Response Zetapotential (nm)

1	Center	-1	-1	0	80.3±0.01	470±0.01	-42.4±0.2
2	IBFact	0	0	0	85.6±0.05	320±0.04	38.6±0.32
3	Center	0	1	1	80.3±0.02	470±0.5	-42.4±0.12
4	IBFact	1	0	-1	81.4±0.5	637±1.2	20.2±0.24
5	IBFact	0	-1	1	92.3±0.06	233±0.03	-62.8±0.26
6	IBFact	-1	0	1	97.3±0.02	432±0.62	-32.6±0.11
7	IBFact	1	1	0	96.9±0.03	186±0.18	-26.2±0.2
8	IBFact	0	0	0	91.2±0.09	450±0.6	-21.3±0.31
9	IBFact	1	0	1	96.6±0.02	250±0.02	-27.2±0.01
10	Center	0	-1	-1	80.3±0.08	470±0.7	-42.4±0.31
11	Center	-1	1	0	80.3±0.5	450±0.62	-30.2±0.11
12	IBFact	-1	0	-1	82.5±0.06	480±0.32	-36.4±0.23
13	IBFact	0	0	0	94.3±0.03	226±0.21	-34.2±0.21
14	Center	0	1	-1	80.3±0.04	470±0.56	-42.4±0.06
15	IBFact	0	0	0	90.3±0.5	242±0.31	-31.2±0.21
16	IBFact	0	0	0	97.7±0.02	272±0.12	-21.6±0.01
17	IBFact	1	-1	0	95.4±0.04	350±0.43	-33.2±0.13

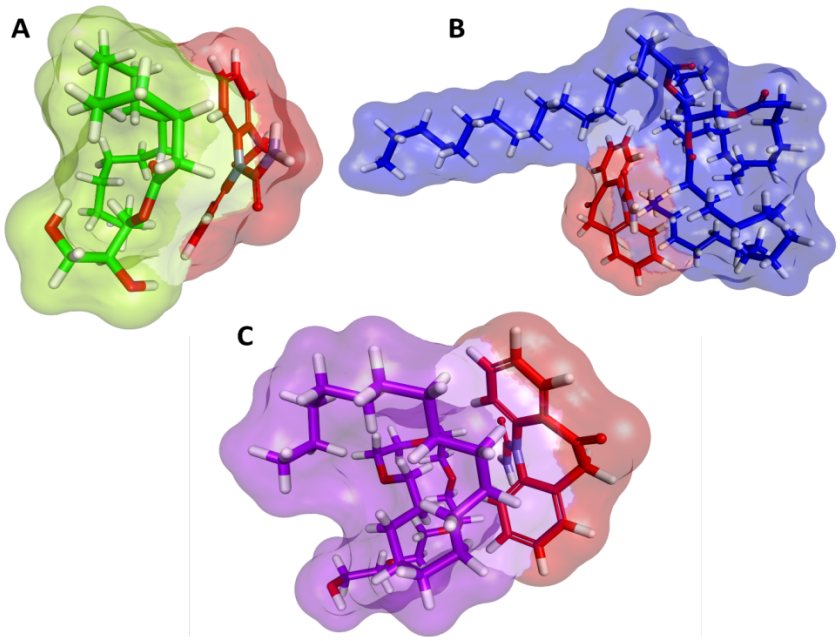

Figure 1: Molecular docking interactions of oxcarbazepine with different pharmaceutical polymers. (A) Binding pose of oxcarbazepine with glycerol monostearate (Geolol surrogate), (B) interaction of oxcarbazepine with tristearin (a glyceryl tristearate analog), and (C) docked complex of oxcarbazepine with PEG-4 Stearyl ether (Brij S 100).

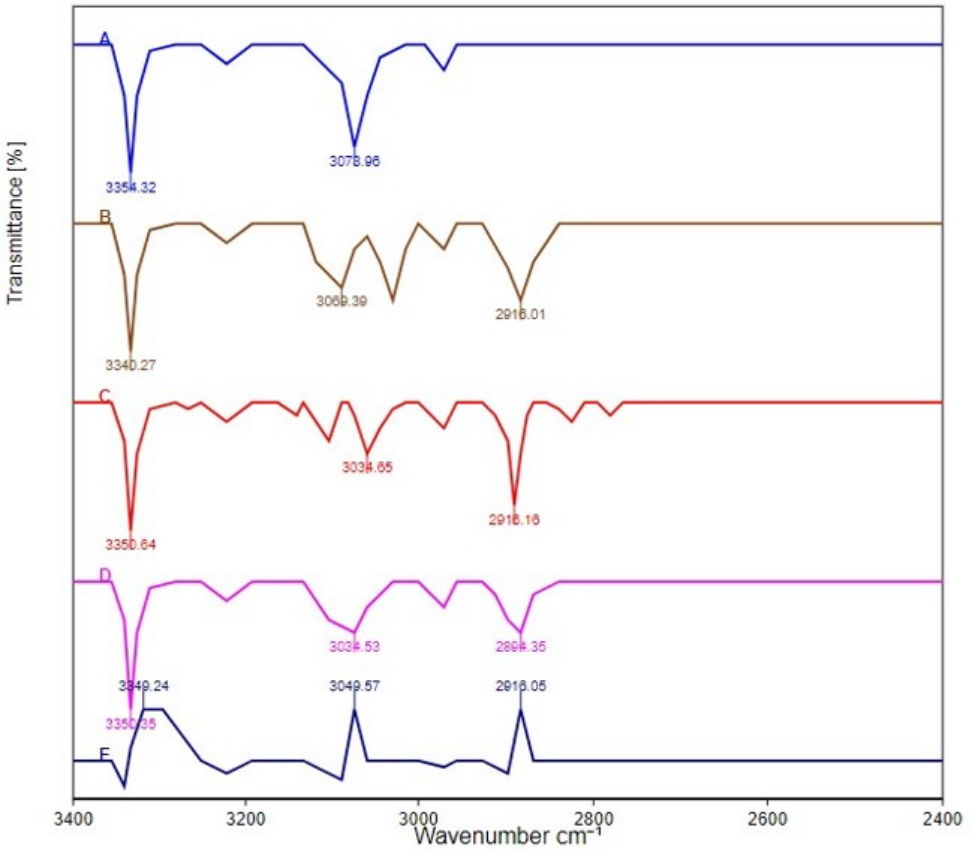

Figure: 2 FTIR Spectra of A) oxcarbazepine, B) oxcarbazepine and glycol mono- and diglycerides, C) oxcarbazepine and glyceryl Trysterate, D) oxcarbazepine and BrijS 100, and E) mixture

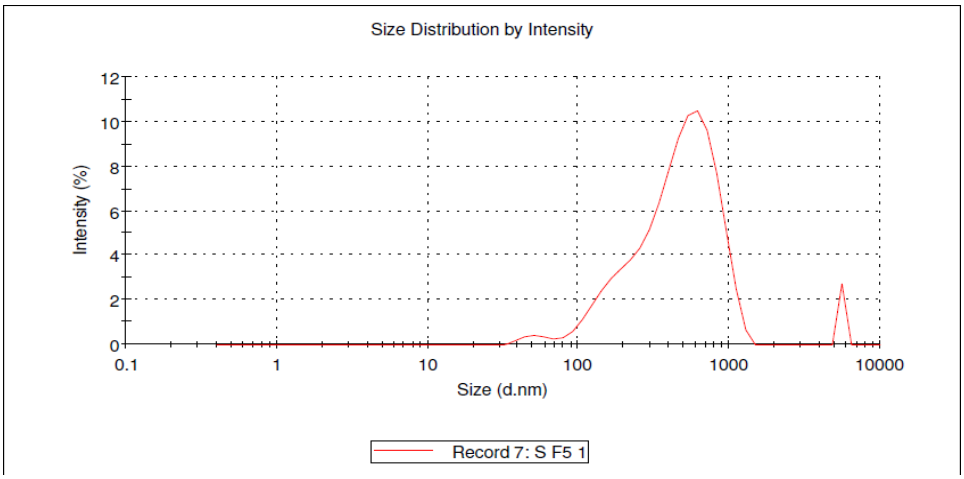

Figure 3: Particle size of the OXZL formulation

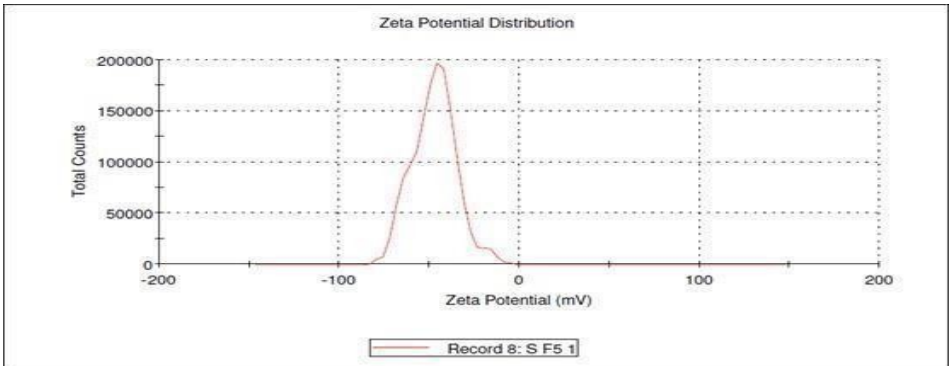

Figure: 4 Zetapotential of the OXZL formulation

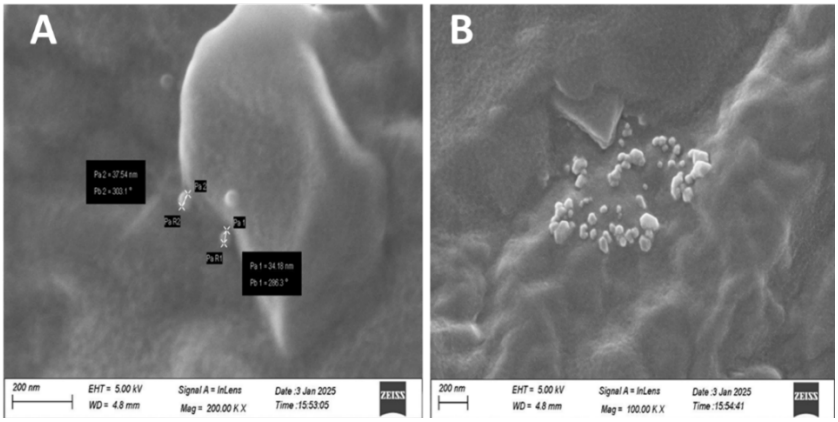

Figure 5 FESEM image revealing that the liposomal structure has a smooth spherical morphology. A: FESEM image of the OXZL formulation at 200 KX B: FESEM image of the OXZL formulation at 1000 KX.

Table 3: Effects of OXZL on PTZ-induced seizures

Treatment group	No. of Convulsion/No. of Animals Used	Onset of the seizure (min)	Duration of the Seizure (min)	Flexion (min)	Extension (min)	Clonus (min)
Normal	0/6	0±0		0±0	0±0	0±0
PTZ treatment	6/3	0.15±0.001	24.3±0.2	3.6±0.2	15.4±0.4	5.3±0.5
PTZ+OXZ treatment	4/0	4.3±0.02	20.3±0.03	2.2±0.3	9.5±0.3	3.2±0.2
PTZ+OXZL treatment	0/6	7.3±0.01	4.5±0.02	0.2±0.1	2.1±0.3	0.3±0.2

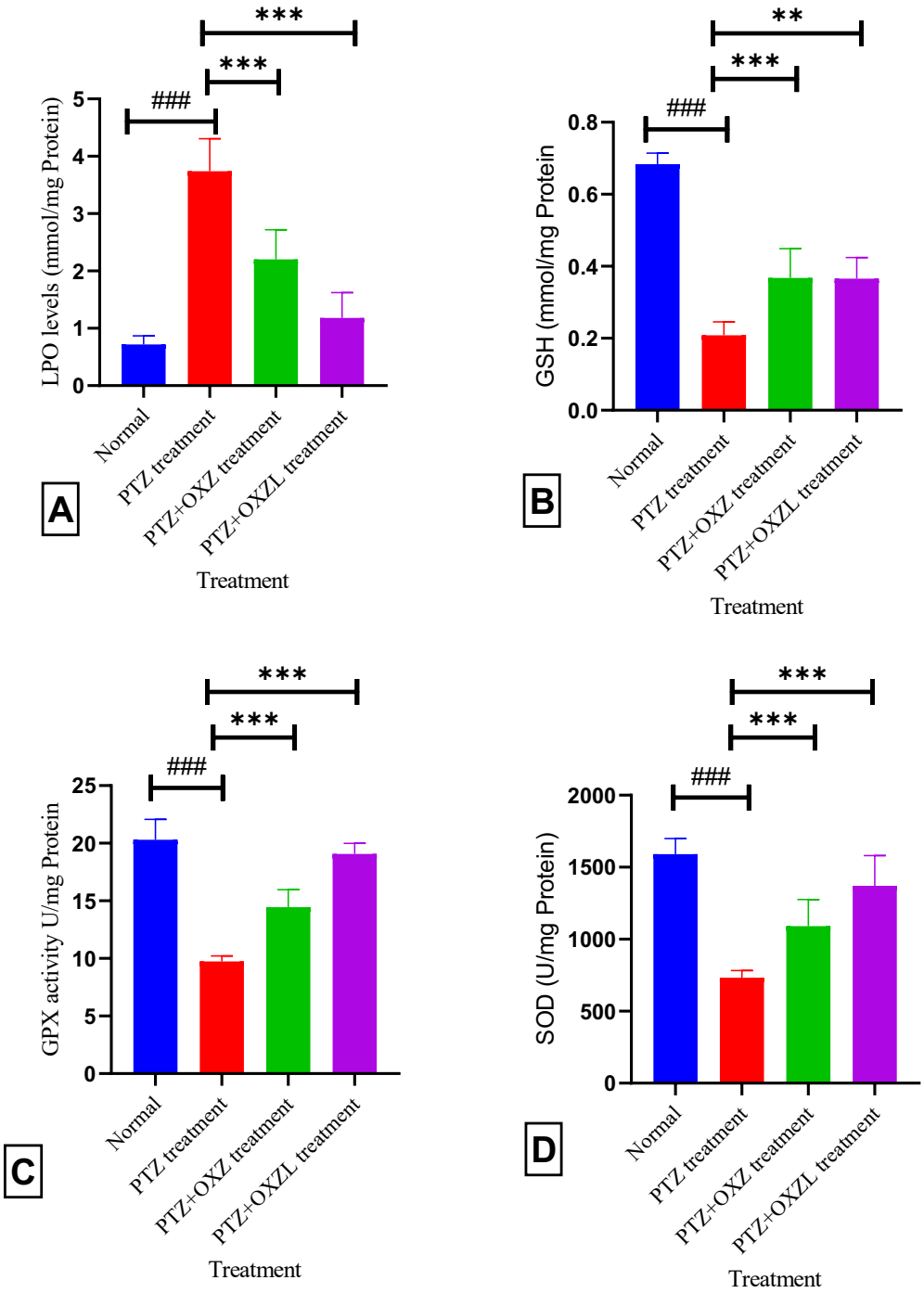

Figure 6 Effects of OXZ and OXZL on brain hippocampus stress parameters. A) LPO activity, B) GSH activity, C) GPx activity, D) SOD activity. All the results are expressed as the means ± SEMs and were analyzed via one-way ANOVA. ### $p < 0.001$, comparison between normal rats and PTZ treatment; ***$p < 0.001$ and **$p < 0.01$ comparison between PTZ treatment and OXZ, OXZL treatment.

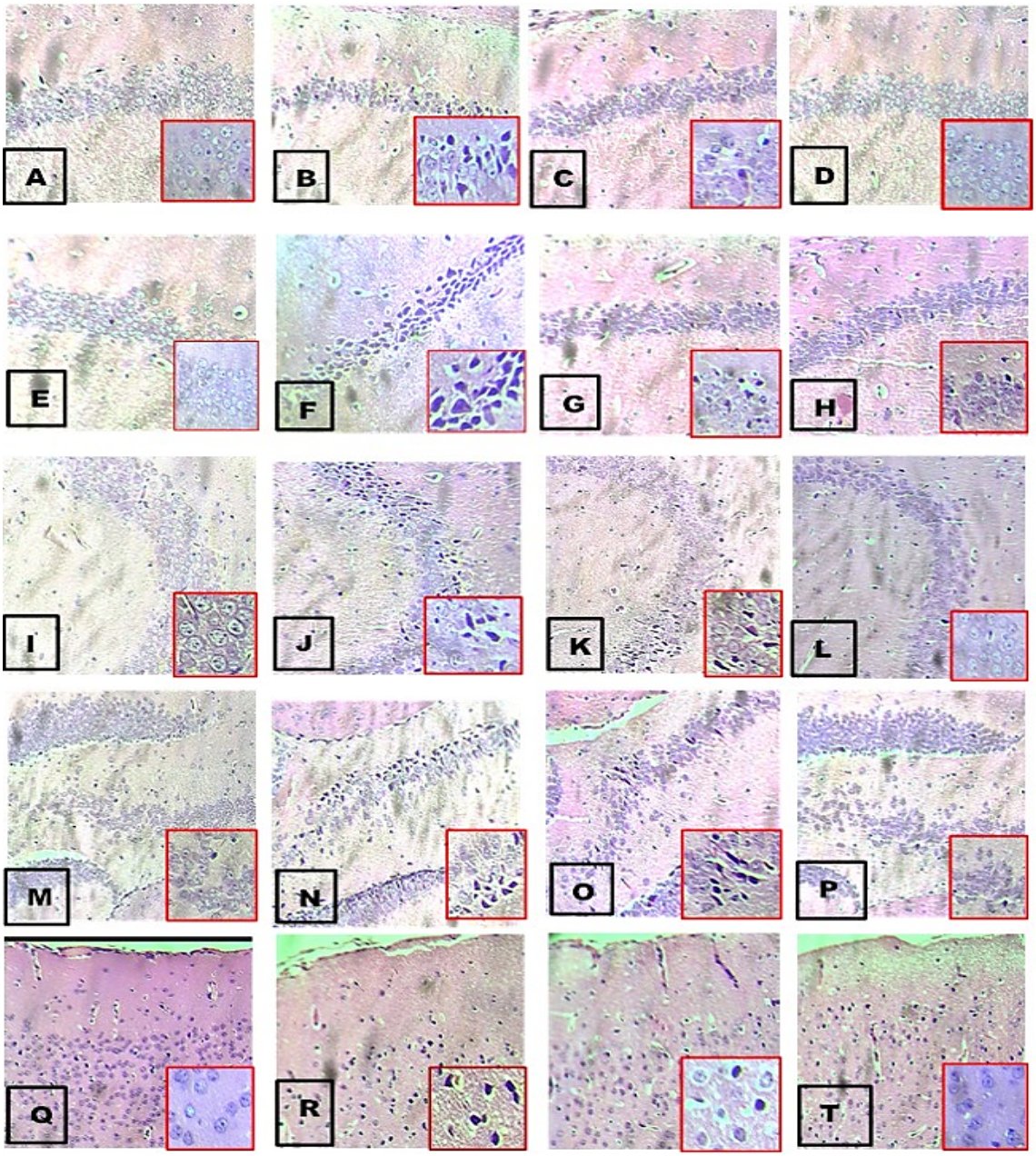

Figure 7 Histology of the CA1 region of the hippocampus. A) Normal mice. B) PTZ treatment. C) PTZ + OXZ treatment. D) PTZ+OXZL treatment. Hippocampal CA2. E) Normal mice. F) PTZ treatment. G) PTZ + OXZ treatment. H) PTZ+OXZL treatment. Hippocampus CA3. I) Normal mice. J) PTZ treatment. K) PTZ + OXZ treatment. L) PTZ+OXZL treatment. Hippocampal DG. M) Normal mice. N) PTZ treatment. O) PTZ + OXZ treatment. P) PTZ+OXZL treatment. Cortex. Q) Normal mice. R) PTZ treatment. S) PTZ + OXZ treatment. T) PTZ+OXZL treatment

6. REFERENCES

[1] Das P, Singh R, Kumar A. Current Scenario and recent advances of Neurological Disorder. J Complement Med Res. 2023;14:110-21.

[2] Beghi E. Addressing the burden of epilepsy: many unmet needs. Pharmacological research. 2016;107:79-84.

[3] Niriayo YL, Gebregziabher T, Demoz GT, Tesfay N, Gidey K. Drug therapy problems and contributing factors among patients with epilepsy. Plos one. 2024;19(3):e0299968.

[4] Reimers A, Brodtkorb E. Second-generation antiepileptic drugs and pregnancy: a guide for clinicians. Expert review of neurotherapeutics. 2012;12(6):707-17.

[5] Kalis MM, Huff NA. Oxcarbazepine, an antiepileptic agent. Clinical therapeutics. 2001;23(5):680-700.

[6] Abou-Taleb BA, El-Ganainy SO. Thermoresponsive gel-loaded oxcarbazepine nanosystems for nose-to-brain delivery: enhanced antiepileptic activity in rats. Pharmaceutical Research. 2023;40(7):1835-52.

[7] Sengar A. Innovations and mechanisms in liposomal drug delivery: A comprehensive introduction. Journal of Emergency Medicine Open Access (J Emerg Med OA). 2025;3(1):01-5.

[8] Nance E, Pun SH, Saigal R, Sellers DL. Drug delivery to the central nervous system. Nature Reviews Materials. 2022;7(4):314-31.

[9] Musumeci T, Bonaccorso A, Carbone C. Basic concepts of liposomes: Components, structures, properties and classification. Liposomes in Drug Delivery: Elsevier; 2024. p. 19-48.

[10] Xiang B, Cao D-Y. Preparation of drug liposomes by thin-film hydration and homogenization. Liposome-based drug delivery systems: Springer; 2021. p. 25-35.

[11] Alshaer W, Nsairat H, Lafi Z, Hourani OM, Al-Kadash A, Esawi E, et al. Quality by design approach in liposomal formulations: Robust product development. Molecules. 2022;28(1):10.

[12] Otto DP. Experimental Designs in Pharmaceutical Formulation Development. Principles of Research Methodology and Ethics in Pharmaceutical Sciences: CRC Press. p. 137-97.

[13] Neri S, Mastroianni G, Gardella E, Aguglia U, Rubboli G. Epilepsy in neurodegenerative diseases. Epileptic Disorders. 2022;24(2):249-73.

[14] Parsons AL, Bucknor EM, Castroflorio E, Soares TR, Oliver PL, Rial D. The interconnected mechanisms of oxidative stress and neuroinflammation in epilepsy. Antioxidants. 2022;11(1):157.

[15] Alkhudhayri A, Abdel Moneim AE, Rizk S, Bauomy AA, Dkhil MA. The neuroprotective effect associated with echinops spinosus in an acute seizure model induced by pentylenetetrazole. Neurochemical Research. 2023;48(1):273-83.

[16] Madireddy S, Madireddy S. Therapeutic strategies to ameliorate neuronal damage in epilepsy by regulating oxidative stress, mitochondrial dysfunction, and neuroinflammation. Brain sciences. 2023;13(5):784.

[17] Pasala PK, Prasanth D, Panda SP, Munnangi V, Blessy S, Ahmad SF, et al. Salacia fruticosa methanol extract pretreatment attenuates scopolamine-induced cognitive decline and Alzheimer's disease-related pathology in zebrafish. Asian Pacific Journal of Tropical Biomedicine. 2025;15(3):109-18. 10.4103/apjtb.apjtb_642_24.

[18] Prasanth DSNBK, Pasala PK, Nithiya P, Yaraguppi DA, Sowjanya P, Sai NB, et al. In-Silico Evaluation of Bioactive Compounds from Tecoma stans (L.) Juss. ex Kunth Flowers for Acid-β-Glucosidase Inhibition in Gaucher's Disease. Chemistry Africa. 2025. 10.1007/s42250-025-01237-9.

[19] Thummala UK, Maddi EG, Avula PR. Optimization of Fast-dissolving Tablets of Ledipasvir-sofosbuvir Inclusion Complexes by Design of Experiments. Indian J Pharmaceut Educ Res. 2023;57(1):33-44.

[20] Thummala UK, Maddi EG, Avula PR. Orodispersible films of Ledipasvir and Sofosbuvir Combination: Formulation optimization and development using Design of Experiments. Asian Journal of Pharmaceutical Research. 2022;12(1):11-8.

[21] Thummala UK, Maddi EG, Avula PR. Optimization and development of orodispersible films for ledipasvir and sofosbuvir through solid dispersion using Box-Behnken design. Research Journal of Pharmaceutical Dosage Forms and Technology. 2021;13(3):201-8.

[22] Yuwanda A, Surini S, Harahap Y, Jufri M. Study of valproic acid liposomes for delivery into the brain through an intranasal route. Heliyon. 2022;8(3).

[23] Ashhar MU, Kumar S, Ali J, Baboota S. CCRD based development of bromocriptine and glutathione nanoemulsion tailored ultrasonically for the combined anti-parkinson effect. Chemistry and Physics of Lipids. 2021;235:105035.

[24] Çağdaş M, Sezer AD, Bucak S. Liposomes as Potential Drug Carrier Systems for Drug. Application of nanotechnology in drug delivery. 2014:1.

[25] Kaklotar D, Agrawal P, Abdulla A, Singh RP, Sonali, Mehata AK, et al. Transition from passive to active targeting of oral insulin nanomedicines: enhancement in bioavailability and glycemic control in diabetes. Nanomedicine. 2016;11(11):1465-86.

[26] Malhotra J, Gupta YK. Effect of adenosine receptor modulation on pentylenetetrazole-induced seizures in rats. British journal of pharmacology. 1997;120(2):282-8.

[27] Abdel-Rahman M, Arafa N, El-khadragy MF, Kassab RB. The neuroprotective role of Nigella sativa extract on ciprofloxacin and pentylenetetrazole treated rats. Afr J Pharm Pharmacol. 2013;7(24):1660-70.

[28] Arafa NM, Abdel-Rahman M, El-khadragy MF, Kassab RB. Evaluation of the possible epileptogenic activity of ciprofloxacin: the role of Nigella sativa on amino acids neurotransmitters. Neurochemical research. 2013;38(1):174-85.

[29] Racine RJ. Modification of seizure activity by electrical stimulation: II. Motor seizure. Electroencephalography and clinical neurophysiology. 1972;32(3):281-94.

[30] Al Omairi NE, Albrakati A, Alsharif KF, Almalki AS, Alsanie W, Abd Elmageed ZY, et al. Selenium Nanoparticles with Prodigiosin Rescue

Hippocampal Damage Associated with Epileptic Seizures Induced by Pentylenetetrazole in Rats. Biology. 2022;11(3):354.

[31] Paglia DE, Valentine WN. Studies on the quantitative and qualitative characterization of erythrocyte glutathione peroxidase. The Journal of laboratory and clinical medicine. 1967;70(1):158-69.

[32] Misra HP, Fridovich I. The role of superoxide anion in the autoxidation of epinephrine and a simple assay for superoxide dismutase. Journal of Biological chemistry. 1972;247(10):3170-5.

[33] Anjali P, Jawahar N, Kumar MP, Jubie S, Selvamuthukumar S. Nanocarriers in the treatment of epilepsy: Challenges and opportunities. Journal of Drug Delivery Science and Technology. 2024;97:105788.

[34] Yang R, Sun Y, Zhao X, Liu W. pH-responsive dissociable liposome/ferritin nanoparticles for treating acute epilepsy through regulating microvascular stabilization and remodeling inflammatory microenvironment. Nano Today. 2025;61:102652.

[35] Li J, Xiao Y, Guo R, Bi Y, Zhang H, Xu X. Enhancing the long-term stability of glyceryl monostearate-based oleogels by incorporating hydroxy monoglyceride as an additional scaffolding agent. LWT. 2024;214:117154.

[36] Barroso NG, Martins AJ, Júnior FD, Okuro PK, Pereira RC, Vicente AA, et al. β-carotene and resveratrol loaded glycerol monostearate-based oleogels: Physicochemical characterization at low gelation concentrations. Food Research International. 2024;197:115181.

[37] Bertoni S, Passerini N, Albertini B. Liquid lipids act as polymorphic modifiers of tristearin-based formulations produced by melting technologies. Pharmaceutics. 2021;13(7):1089.

[38] Gagliardi A, Voci S, Salvatici MC, Fresta M, Cosco D. Brij-stabilized zein nanoparticles as potential drug carriers. Colloids and Surfaces B: Biointerfaces. 2021;201:111647.

[39] Pande S. Liposomes for drug delivery: review of vesicular composition, factors affecting drug release and drug loading in liposomes. Artificial Cells, Nanomedicine, and Biotechnology. 2023;51(1):428-40.

[40] Zade D. Advances in Targeted Drug Delivery Systems for Cancer Therapy: Nanotechnology to Clinical Translation. Journal of Drug Delivery and Biotherapeutics. 2025;2(3):55-9.

[41] Khan JZ, Zainab SR, Rehman MU, Abid M, Mazhar MU, Shah FA, et al. Chronic stress intensify PTZ-induced seizures by triggering neuroinflammation and oxidative stress. Biochemical and Biophysical Research Communications. 2024;729:150333.

[42] Agrawal SS, Baliga V, Londhe VY. Liposomal formulations: A recent update. Pharmaceutics. 2024;17(1):36.

[43] Osuntokun OS, Abdulwahab UF, Akanji NO, Adedokun KI, Adekomi AD, Olayiwola G. Anticonvulsant and neuroprotective effects of carbamazepine-levetiracetam adjunctive treatment in convulsive status epilepticus rat model: Inhibition of cholinergic transmission. Neuroscience Letters. 2021;762:136167.

[44] Althagafi HA. Neuroprotective role of chlorogenic acid against hippocampal neuroinflammation, oxidative stress, and apoptosis following acute seizures induced by pentylenetetrazole. Metabolic Brain Disease. 2024;39(7):1307-21.

[45] Demyashkin G, Blinova E, Grigoryan M, Parshenkov M, Skovorodko P, Ius V, et al. Neuroprotective effects of myricetin on PTZ-Induced seizures in mice: evaluation of oxidation, neuroinflammation and metabolism, and apoptosis in the Hippocampus. Current Issues in Molecular Biology. 2024;46(8):8914.